# STUDY OF DENSITY WAVE PHENOMENA IN BOILING AND CONDENSING TWO-PHASE FLOW SYSTEMS

Ruspini, L.C.<sup>a,1</sup>, Dorao, C.A.<sup>a</sup>, Fernandino, M.<sup>a</sup>

<sup>a</sup>Department of Energy and Process Engineering. Faculty of Engineering Science and Technology, Norwegian University of Science and Technology leonardo.c.ruspini@ntnu.no

#### **Abstract**

In this work density wave oscillations are studied. This phenomenon have been widely studied for boiling systems with sub-cooled inlet condition in the past. The main purpose of this work is to characterize the stability region of boiling and condensing systems for sub-cooled and saturated inlet conditions. Stability maps, based on the sub-cooling and the phase-change numbers, are constructed. The limits of the unstable regions are identified and characterized. Finally some numerical simulations are presented in order to describe the nature of the involved phenomena. A high-order numerical solver, based on a homogenous two-phase model for a single boiling channel is implemented.

#### 1. Introduction

The departure from a stable operation condition can cause severe damages in many industrial systems, such as heat exchangers, nuclear reactors, re-boilers, steam generators, thermal-siphons, etc. Oscillations and instabilities induced by boiling two-phase flows are of relevance for the design and operation of these systems. For this reason, the stability in thermal-hydraulic variables such as flow, pressure and temperature should be studied in detail to better understand and characterize the conditions for the occurrence of these phenomena.

Several aspects of density wave phenomena boiling systems with sub-cooled inlet conditions have been thoroughly discussed in the literature, both theoretically and experimentally [11, 10, 22, 23, 25, 15, 14, 1]. Moreover in the last 20 years several works present a critical discussion to the traditional description of density wave that clarifies the nature and the involved mechanisms taking place in the occurrence of this phenomenon for different sub-cooling conditions [18, 17, 2]. According to these works, the mechanisms responsible of the oscillatory behavior are the change in the exit density, related with the slope of the density profile, and the change of the exit flow. For different sub-cooling those effects have a stronger or weaker influence over the system.

However it is still not clear how the density wave mechanisms affect the systems for condensing and saturated boiling flows. In [13] an experimental example and some numerical simulations show the occurrence of oscillations in the condensing secondary side of a heat exchanger, stating that condensation processes are similar to the boiling processes in sense of occurrence of density wave oscillations. However no theoretical analysis is presented to support the previous statement. Moreover several works describe the occurrence of oscillations in condensing system [4, 5, 16, 6]. According to these experimental works the nature of the oscillations seems to be very different from density waves phenomena, regarding time periods.

<sup>&</sup>lt;sup>1</sup>Tel: +47 73595352, Fax: +47 73593491.

Table 1: Nomenclature

Lowercase	G	mass flux
specific enthalpy	K	valve constant
Darcy friction factor	L	pipe length
time coordinate	P	pressure
specific volume	$P_H$	wet perimeter
themodynamic quality	Q	constant heat source
space coordinate	T	temperature
density		
Uppercase	<b>Subscripts</b>	
cross section area	in	inlet
hydraulic diameter	out	outlet
	specific enthalpy Darcy friction factor time coordinate specific volume themodynamic quality space coordinate density Uppercase cross section area	$ \begin{array}{cccccccccccccccccccccccccccccccccccc$

The purpose of this work is to use the knowledge developed for boiling systems with sub-cooled inlet condition, in order to understand how the mechanisms involved in density wave phenomenon affect condensing and boiling systems with saturated inlet conditions . A homogeneous model is presented to study the nature of these different phenomena for different operation regions. Non-dimensional stability maps,  $N_{pch}\ vs\ N_{sub}$ , are constructed and several simulations show the behavior of a simple thermal-hydraulic system. In addition the application of a high-order method to solve the conservation equations is described and implemented.

#### 2. Model

The thermo-hydraulic system used to study this kind of instabilities consists of two constant pressure tanks, two valves and a heated section, as shown in Figure 1. In this model, the pressure difference between both tanks acts as the driving force (external characteristic) and, according to the  $K_{in}$  valve opening, the external characteristic results in a quadratic decreasing curve. The implemented model is based on the following assumptions,

- One-dimensional model.
- Thermodynamic equilibrium conditions.
- Two-phase homogeneous model [15].
- Colebrook pressure drop correlation in the single phase region and two-phase Müller-Steinhagen and Heck pressure drop correlation for two-phase flow region [24].

The mathematical model used to describe the thermal-hydraulic evolution of the heated section is based on the mass, momentum and energy conservation. They can be expressed as

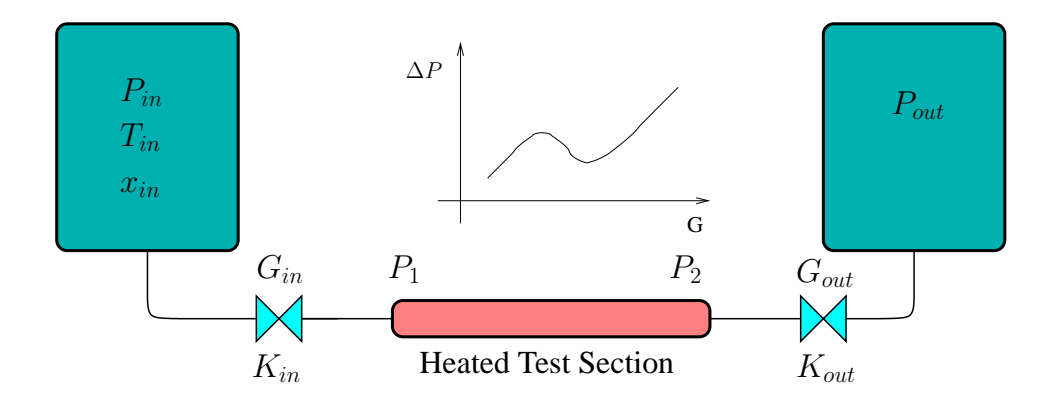


Figure 1: Scheme of the implemented model.

$$\frac{\partial \rho}{\partial t} + \frac{\partial G}{\partial z} = 0 \tag{1}$$

$$\frac{\partial G}{\partial t} + \frac{\partial}{\partial z} \left( \frac{G^2}{\rho} \right) + \frac{\partial P}{\partial z} + \left[ \frac{f}{D_H} + \sum_{i=1}^{N} K_i \delta(z - z_i) \right] \frac{G^2}{2\rho} = 0$$
 (2)

$$\frac{\partial \rho h}{\partial t} + \frac{\partial Gh}{\partial z} = Q \frac{P_H}{A_{rs}} \tag{3}$$

The pressure drop in the valves is calculated using a homogeneous pressure drop concentrated value,  $K_i$ , for each valve (in, out). Friction losses are neglected in the energy equation. Finally the friction factor; f in Eq. (2) is given by the known Colebrook correlation for the single phase regions, liquid or gas, and by the Müller-Steinhagen and Heck correlation for the two-phase region [24]. In contrast with previous models, in this work the profile of density is updated according to the local enthalpy and pressure. For this updating a thermodynamic equilibrium is assumed.

### 3. Numerical approximation

The introduction of a significant diffusion by low-order methods can modify the nature of the problem. High-order discretization reduces the numerical diffusion. The necessity of solving thermal-hydraulic problems with accurate methods was analyzed in [3, 20], where the numerical aspects of the implementation of this kind of problems are fully described. More details about the implementation of this numerical solver can be found in [19, 21].

In a general case the least squares formulation is based on the minimization of a norm—equivalent functional. For simplicity, the system of equations can be represented as

$$\mathcal{L}\mathbf{u} = \mathbf{g} \quad in \ \Omega \tag{4}$$

$$\mathcal{B}\mathbf{u} = \mathbf{u}_{\Gamma} \quad on \ \Gamma \subset \partial\Omega \tag{5}$$

with  $\mathcal{L}$  a linear partial differential operator and  $\mathcal{B}$  the trace operator. We assume that the system is well–posed and the operator  $(\mathcal{L},\mathcal{B})$  is a continuous mapping between the function space  $X(\Omega)$  onto the space  $Y(\Omega) \times Y(\Gamma)$ . The norm equivalent functional becomes

$$\mathcal{J}(\mathbf{u}) \equiv \frac{1}{2} \parallel \mathcal{L}\mathbf{u} - \mathbf{g} \parallel_{Y(\Omega)}^{2} + \frac{1}{2} \parallel \mathcal{B}\mathbf{u} - \mathbf{u}_{\Gamma} \parallel_{Y(\Gamma)}^{2}$$
 (6)

Based on variational analysis, the minimization statement is equivalent to:

$$\lim_{\epsilon \to 0} \frac{d}{d\epsilon} \mathcal{J}(\mathbf{u} + \epsilon \, \mathbf{v}) = 0 \quad \forall \, \mathbf{u} \in X(\Omega)$$
 (7)

Hence, the necessary condition for the minimization of  $\mathcal J$  is equivalent to: Find  $f\in X(\Omega)$  such that

$$\mathcal{A}(\mathbf{u}, \mathbf{v}) = \mathcal{F}(\mathbf{v}) \quad \forall \mathbf{v} \in X(\Omega)$$
(8)

with

$$\mathcal{A}(\mathbf{u}, \mathbf{v}) = \langle \mathcal{L}\mathbf{u}, \mathcal{L}\mathbf{v} \rangle_{Y(\Omega)} + \langle \mathcal{B}\mathbf{u}, \mathcal{B}\mathbf{v} \rangle_{Y(\Gamma)}$$
(9)

$$\mathcal{F}(\mathbf{v}) = \langle \mathbf{g}, \mathcal{L}\mathbf{v} \rangle_{Y(\Omega)} + \langle \mathbf{u}_{\Gamma}, \mathcal{B}\mathbf{v} \rangle_{Y(\Gamma)}$$
(10)

$$\mathcal{A}(\mathbf{v}_h, \mathbf{v}_h)\mathbf{u}_h = \mathcal{F}(\mathbf{v}_h) \quad \forall \mathbf{v}_h \in X_h(\Omega_h)$$
(11)

where  $A: X \times X \to \mathbb{R}$  is a symmetric, continuous bilinear form, and  $\mathcal{F}: X \to \mathbb{R}$  a continuous linear form. The introduction of the boundary residual allows the use of spaces  $X(\Omega)$  that are not constrained to satisfy the boundary conditions. The boundary terms can be omitted and the boundary conditions must be enforced strongly in the definition of the space  $X(\Omega)$ . Finally, the searching space is restricted to a finite dimensional space such that  $\mathbf{u}_h \in X_h(\Omega) \subset X(\Omega)$ .

# 3.1. Numerical description of the problem

From Eqs. (1-3) it is possible to see that the system is highly non-linear. For that reason it is necessary to find a linear form for this set of equations in order to use LSSM (Least Square Spectral Method). Non-linear effects are considered by implementing an iterative Picard loop. Hence, using the operator description of Eq. (4), it is possible to rewrite the linearized system, described in Eqs. (1-3), as

$$\mathcal{L} = \begin{cases} \frac{\partial \bullet}{\partial z} & 0 & 0 \\ \frac{\partial \bullet}{\partial t} & \frac{\partial \bullet}{\partial z} & 0 \\ 0 & 0 & \rho^* \frac{\partial \bullet}{\partial t} + G^* \frac{\partial \bullet}{\partial z} \end{cases}$$
(12)

$$\mathbf{g} = \left\{ \begin{array}{c} -\frac{\partial}{\partial z} \rho^* \\ -\frac{\partial}{\partial z} \left( \frac{G^{*2}}{\rho^*} \right) - \left[ \frac{f}{D_H} + \sum_{i}^{N} K_i \delta(x - x_i) \right] \frac{G^{*2}}{2\rho^*} \\ Q \frac{P_H}{A_{xs}} \end{array} \right\}$$
(13)

$$\mathbf{u} = \left\{ \begin{array}{c} G \\ P \\ h \end{array} \right\} \tag{14}$$

where  $G^*$  and  $\rho^*$  correspond to the old values of flow and density in the non-linear loop. The operator  $\mathcal B$  is the matrix where the corresponding initial and boundary nodes are set to one and the  $\mathbf u_\Gamma$  corresponds to the initial values for flow, pressure and enthalpy. Boundary conditions for enthalpy and pressure are added to the boundary vector  $\mathbf u_\Gamma$  at x=0 and the third boundary condition is set in  $\mathbf u_\Gamma$  at x=L.

## 3.2. Spectral element approximation

The computational domain  $\Omega$  is divided into  $N_e$  non-overlapping sub-domains  $\Omega_e$  of diameter  $h_e$ , called spectral elements, such that

$$\Omega = \bigcup_{e=1}^{N_e} \Omega_e, \qquad \Omega_e \cap \Omega_l = \emptyset, \quad e \neq l$$
(15)

The global approximation in  $\Omega$ ,  $\mathbf{u}_h$ , is constructed by gluing the local approximations  $\mathbf{u}_h^e$ , i.e.

$$\mathbf{u}_h = \bigcup_{e=1}^{N_e} \mathbf{u}_h^e \tag{16}$$

The local approximation solution  $\mathbf{u}_h^e$  can be expressed like

$$\mathbf{u}_{h}^{e}(x,t) = \sum_{i=0}^{N_{1}} \sum_{i=0}^{N_{2}} u_{ij}^{e} \, \varphi_{i}(x) \, \varphi_{j}(t), \quad \text{with } u_{ij}^{e} = u(x_{i}, t_{j})$$
(17)

where  $\varphi_i(x)$  and  $\varphi_j(t)$  are the one dimensional basis functions. The basis functions used in this work are the Lagrangian interpolants polynomials through the Gauss–Lobatto–Legendre (GLL) collocation points, see [7].

## 4. Stability analysis

The system stability is analyzed by the construction of a non-dimensional stability map. In this work the sub-cooling and phase-change (Zuber) numbers are used [11]. They correspond with

$$N_{sub} = \frac{h_f - h_{in}}{h_{fg}} \frac{\rho_{fg}}{\rho_g} \qquad N_{pch} = \frac{Q}{GA_{xs}h_{fg}} \frac{\rho_{fg}}{\rho_g}$$
 (18)

To evaluate the stability of the numerical solution the evolution of the inlet flow is fitted with the function,

$$f(t) = Ae^{-\alpha t}\sin(\beta t + \gamma) + B \tag{19}$$

then the stability criteria corresponds with

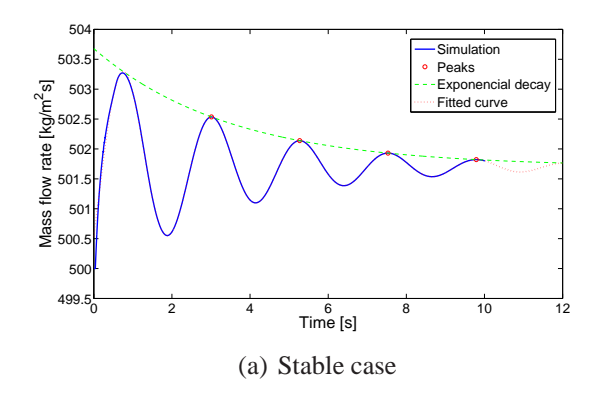
$$\alpha > 0$$
 Stable  $\alpha < 0$  Unstable (20)

Figure 2 shows two different simulations and its corresponding fitted curve, Eq. (19). These simulations correspond respectively with a stable and an unstable cases. For these two cases the  $(N_{pch}, N_{sub})$  pairs are (5.2, 1.1) and (10, 0.6) respectively.

# 5. Numerical results

All the simulations in this work are done in a system with the following characteristics:

- Fluid: R134a
- L = 1m,  $D_H = 5$ mm



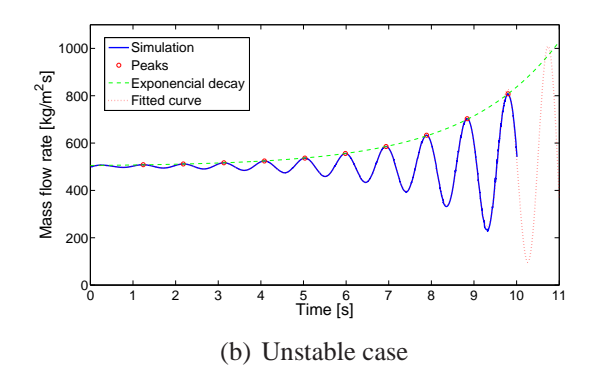


Figure 2: Density wave oscillations and fitted functions. The  $(N_{pch}, N_{sub})$  for each case is: (a) (5.2, 1.1) and (b) (10, 0.6).

- $P_{out} = 8 \cdot 10^5 \text{ Pa}, P_{in} = P_{stationary}(G_{in} = 500 \text{ [kg/m}^2\text{s]})$
- $K_{in} = 2$ ,  $K_{out} = 1$

The numerical order of approximation of time and space is 4. The number of elements in which the space is discretized is  $N_e = 50$  and the time step is  $\Delta t = 10^{-2}$  sec for all the cases. The non-linear relative error tolerance for the Picard loop is  $10^{-6}$ .

# 5.1. Boiling region

As defined by Eq. (18), the boiling region is defined where  $N_{pch}$  is positive. Using the criteria presented on Eq. (20), a stability map of  $\alpha$  as a function of  $(N_{pch},N_{sub})$  is constructed. A total number of 355 simulations are used. In Figure 3 a view of the three-dimensional stability function  $\alpha$  is plotted. For low negative sub-cooling numbers  $(N_{sub} < -5)$  the system response becomes stable very fast  $(\alpha >> 1)$ . This region corresponds with a high-saturated (x > 0.5) or over-heated inlet condition. The high stability of this region is due to the low density change from the saturated to the over-heated states. In contrast for  $(N_{sub} > -5)$  the stability of the system decreases and in some regions  $\alpha$  becomes negative. The stability of the low saturated and sub-cooled region is analyzed in the next sections.

## Saturated region

In Figure 4 the stability map of the saturated region is presented. This region is characterized by a low stability and an unstable behavior. In general terms, the tendency of the stability limit follow the same trend as in the low part of the sub-cooled region ( $N_{sub}>0$ ). When the outlet reaches the single phase gas conditions, red line on Figure 4, the stability limit suffers an inflection point. This change of behavior corresponds to the difference in the local pressure drop at the exit restriction between the single gas and the two-phase cases.

Even when any other work analyzes oscillations in the saturated inlet region, it is necessary to remark its importance since there is a great number of industrial systems that works in saturated conditions with a low amount of vapor. In addition the observed oscillations are much faster than those for high sub-cooling, making it harder for the controlling systems. Moreover any correlation [11, 22, 9], is able to predict the position of these limit.

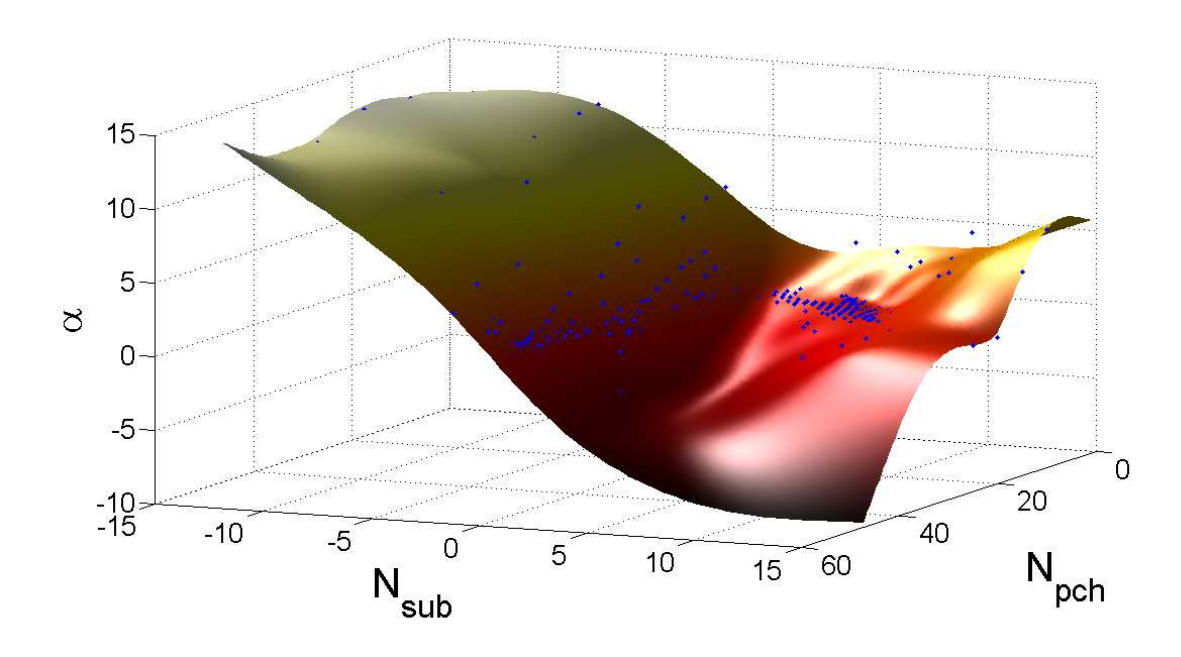


Figure 3: Stability map of  $\alpha$  as a function of  $(N_{pch}, N_{sub})$ . The blue points correspond with the simulations.

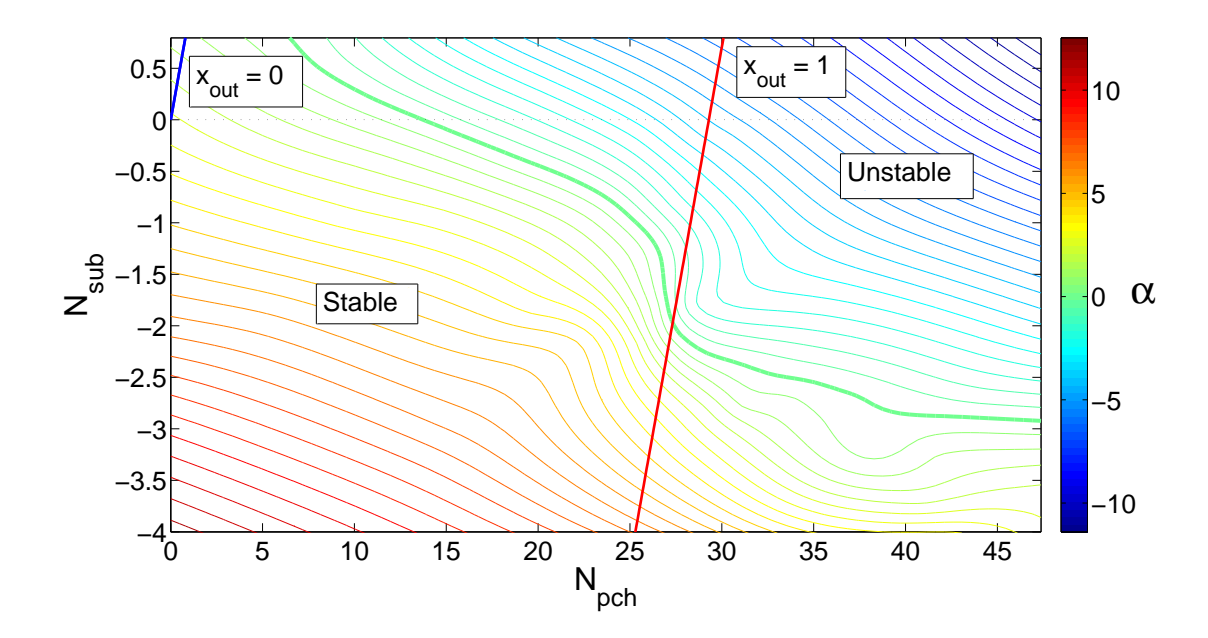


Figure 4: Stable and unstable regions for the saturated case. Green line shows the stability limit for  $\alpha = 0$ .

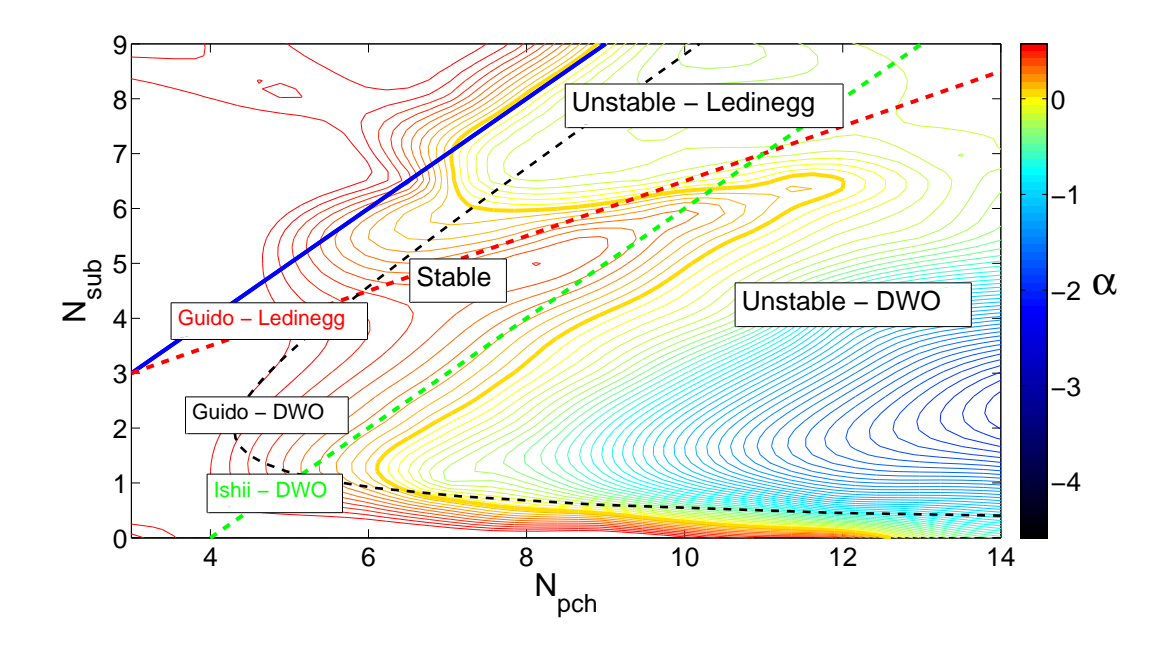


Figure 5: Stable and unstable regions for the sub-cooled case. Ochre line shows the stability limit for  $\alpha = 0$ . Ishii [11] and Guido [9] are also plotted in the map.

## Sub-cooled region

The stability map for the sub-cooled region is presented in Figure 5. In this plot instabilities due to Ledinegg excursions and density wave oscillations (DWO) are observed. For the cases of Ledinegg excursion  $\alpha$  is imposed to  $\alpha=-0.1$  and no fitting is made. An example of Ledinegg excursion is plotted in Figure 6. The classical limit presented by Guido [9] for Ledinegg instability, red line in Figure 5, does not seem to fit the boundary found in this work, for any sub-cooled region. This is probably due to the simplifications, such as not friction in the pipe, used in Guido's lumped model. In addition the DWO limit presented by Guido does not seem either to predict accurately the unstable limit for DWO. In contrast the simplified correlation presented by Ishii [11] seems to predict more accurately the limit of stability for DWO. Nevertheless the differences between Ishii's correlation and the limit obtained in this work could be due to the density profile used in present model. In contrast with Ishii's model, where the liquid density and vapor density are assumed constant, in this work the density profile of the fluid, in the single- and two-phase regions, is updated according to the local enthalpy and pressure.

# 5.2. Condensing region

An example of the response of condensing systems is presented in Figure 7. In this case, in contrast with the behavior of a boiling system, the system evolves in an over-dumped fashion. An exponential curve is fitted as it is shown in Figure 7. The stability map for the condensation region is presented in Figure 8. For all the cases the system behaves in a stable fashion,  $\alpha > 0$ . Moreover the minimum value for the parameter  $\alpha$  is 3.5, Figure 8. A total of 250 cases have been simulated in order to obtain the stability map for condensing systems. In this stability map the cases of  $N_{sub}$  between 2 and -50 are analyzed. The region with positive sub-cooling number is not analyzed since it is the just liquid region.

As described in [18] for the sub-cooled inlet conditions, density wave oscillations are the consequence of the regenerative feedback between friction and delay effects. Note that even when inertia effects are

important [14], they do not define the nature of the oscillation. In general terms it is well known that friction losses at the inlet valve stabilize the system while the outlet friction losses destabilize the system. In addition, it is also known that the variations in the flow and density at the exit control the oscillation occurrence. Since it is imposed a constant pressure to the system, while changes on density produce a positive feedback (unstabilizing), the changes on the exit flow tend to stabilize the system (stabilizing), [18].

Furthermore density profile slopes of opposite sign will affect the system in opposite way, since the same perturbation will produce an opposite reaction in the two-phase friction losses at the exit. For example, in the case of positive slope (cooling) any increase in the flow produces a decrease in the density at the outlet, while in the case of negative slope (heating) any increase of the flow produces an increase in the exit density. In Figure 9 the density profiles for the boiling (heating) and condensing (cooling) cases are presented. For these cases the gradient of the density profile monotonously fulfills

$$\frac{\partial \rho}{\partial z} < 0 \qquad \text{(Heating case)}$$

$$\frac{\partial \rho}{\partial z} > 0 \qquad \text{(Cooling case)}$$
(21)

$$\frac{\partial \rho}{\partial z} > 0$$
 (Cooling case) (22)

note that the last statement is valid for any distribution of heat and any condition at the inlet (sub-cooled, saturated or over-heated). Consequently due to the characteristic positive slope of the density profile for condensing flows, the outlet two-phase friction terms have a stabilizer effect. Thus the system becomes stable in terms of density wave oscillations, as shown by the simulations of condensing systems on Figure 8. This last conclusion is also in accordance with the experimental data reported in [4, 5], where it is shown that the oscillations in condensing systems are not according with density waves and seems to be related with the amount of compressible volume in the system such as pressure drop oscillations for boiling systems [12, 8].

#### 6. Conclusion

Density wave phenomena are analyzed for a boiling or condensing single tube. Density wave oscillations are observed just for boiling flows with saturated and sub-cooled inlet conditions. None of the stability

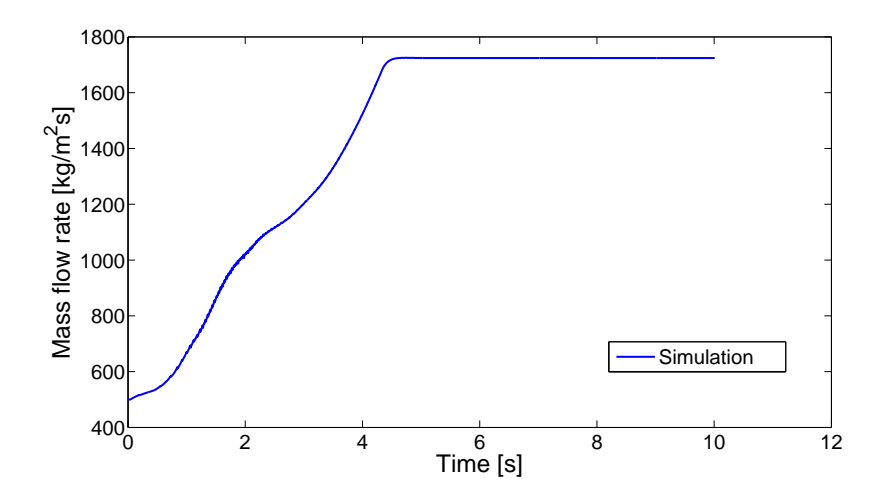


Figure 6: Transient response of the system in a Ledinegg flow excursion. In this case  $(N_{sub}, N_{pch})$  are (7,8).

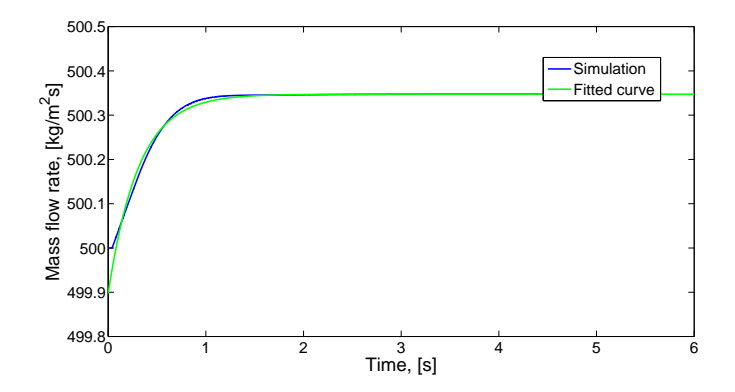


Figure 7: Transient response of the condensing system. This case corresponds to  $(N_{pch}, N_{sub}) = (-30, -2)$ .

correlations for the occurrence of density waves describe the occurrence of these phenomena in the saturated case. The occurrence Ledinegg instabilities is also reported. The limits for stability region are also characterized and a significant difference between those limits and the classical lumped models is observed. No unstable oscillatory behavior is observed for condensing flows. A discussion of the occurrence of density waves in condensing systems is presented. Therefore it is found that due to the characteristic positive slope of the density profile it is not possible to find this phenomenon in condensing flows.

#### 7. References

[1] J.-L. Achard, D. Drew, and R. Lahey. The analysis of nonlinear density-wave oscillations in boiling channels. *J. Fluid Mechanics*, 155:213–232, 1985.

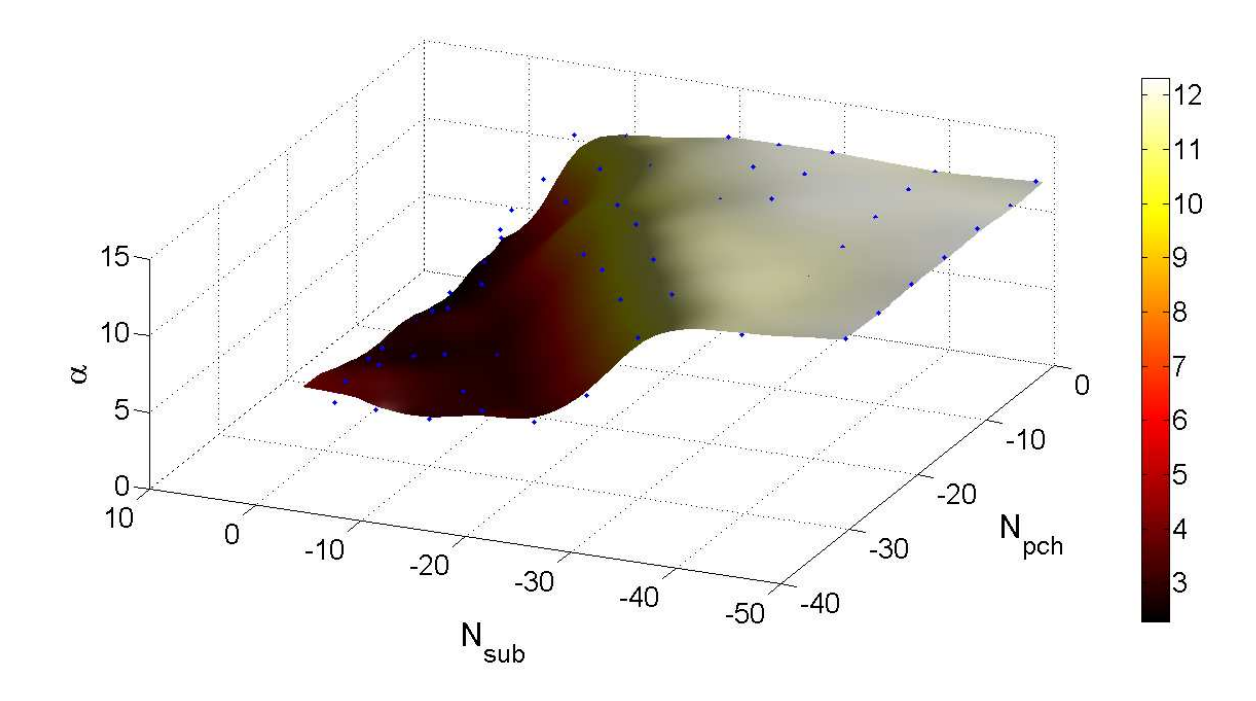


Figure 8: Stability map of  $\alpha$  as a function of  $(N_{pch}, N_{sub})$ . In all the cases  $\alpha$  is positive and then the system is stable. The blue points correspond with the simulations.

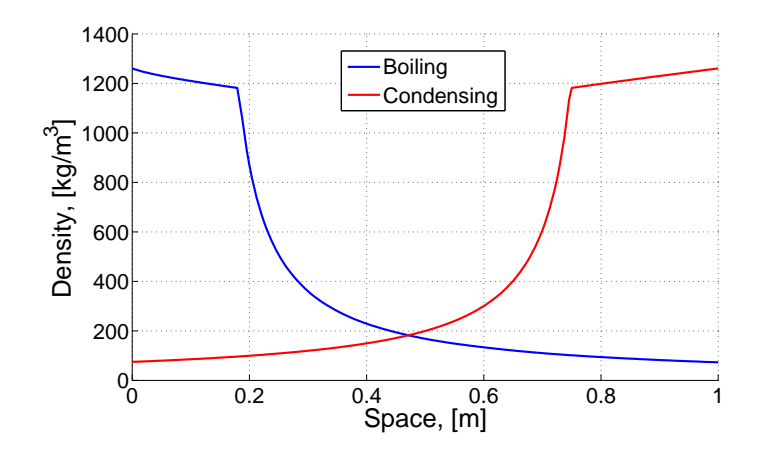


Figure 9: Density profiles for boiling and condensing cases. Boiling case ( $N_{pch} = 19, N_{sub} = 5$ ); Condensing ( $N_{pch} = -19, N_{sub} = -15$ ).

- [2] W. Ambrosini, P. Di Marco, and J. Ferreri. Linear and nonlinear analysis of density wave instability phenomena. *International Journal of Heat and Technology*, 18:27–36, 2000.
- [3] W. Ambrosini and J. Ferreri. The effect of truncation error in the numerical prediction of linear stability boundaries in a natural circulation single phase loop. *Nuclear Engineering and Design*, 183(1-2):53–76, 1998.
- [4] B. Bhatt and G. Wedekind. A self sustained oscillatory flow phenomenon in two-phase condensing flow system. *ASME Journal of Heat Transfer*, 102:695–700, 1980.
- [5] B. Bhatt, G. Wedekind, and K. Jung. Effects of two-phase pressure drop on the self-sustained oscillatory instability in condensing flows. *ASME Journal of Heat Transfer*, 111:538–545, 1989.
- [6] B. Boyer, G. Robinson, and T. Hughes. Experimental investigation of flow regimes and oscillatory phenomena of condensing steam in a single vertical annular passage. *Int. Journal of multiphase flow*, 21:61–74, 1995.
- [7] M. Deville, P. Fisher, and E. Mund. High-order methods for incompressible fluid flow. *Cambridge University Press.*, 2002.
- [8] Y. Ding, S. kakac, and X.J.Chen. Dynamic instabilities of boiling two-phase flow in a single horizontal channel. *Experimental Thermal and Fluid Science*, 11:327–342, 1995.
- [9] G. Guido, J. Converti, and A. Clausse. Density wave oscillations in parallel channels an analytical approach. *Nuclear engineering and Design*, 125:121–136, 1991.
- [10] M. Ishii. *Thermally induced flow instabilities in two-phase mixtures in thermal equilibrium.* PhD thesis, Georgia Institute of Technology, Michigan, 1971.
- [11] M. Ishii and N.Zuber. Thermally induced flow instabilities in two-phase. *Proceedings of the forth international heat transfer metting*, 1970.
- [12] S. Kakac and B. Bon. A review of two-phase flow dynamic instabilities in tube boiling systems. *Int. Journal Heat Mass Tranfer*, 51:399–433, 2007.

- [13] N. I. Kolev. Multiphase Flow Dynamics 4: Nuclear Thermal Hydraulics". Springer.
- [14] R. Lahey. Advances in the analytical modeling of linear and nonlinear density-wave instability modes. *Nuclear Engineering and Design*, 95:5–34, 1986.
- [15] R. Lahey and M. Podoski. On the analysis of varius instabilities in two-phase flows. *Multiphase Science and Technology*, pages 183–370, 1989.
- [16] N. S. LIAO and C. C. WANG. Transient response characteristics of two-phase condensing flows. *Int. J. Multiphase Flow*, 16:139–151, 1990.
- [17] U. Rizwan. Effects of double-humped axial heat flux variation on the stability of two phase flow in heated channels. *Int. J. Multiphase flow*, 20:721–737, 1994.
- [18] U. Rizwan. On density wave oscillations in two-phase flows. *Int. J. Multiphase flow*, 20:721–737, 1994.
- [19] L. Ruspini, C. Dorao, and M. Fernandino. Dynamic simulation of ledinegg instability. *Journal of Natural Gas Science and Engineering*, 2:211–216, 2010.
- [20] L. Ruspini, C. Dorao, and M. Fernandino. Simulation of a natural circulation loop using a least squares hp-adaptive solver. *Mathematics and Computers in Simulation*, 2010.
- [21] L. Ruspini, C. Dorao, and M. Fernandino. Modeling of dynamic instabilities in boiling systems. *Proceedings of 19th International Conference On Nuclear Engineering, ICONE19*, 2011.
- [22] P. Saha, M. Ishii, and N.Zuber. An experimental investigation of the thermally induced flow oscillations in two-phase systems. *Transactions of the ASME*, 1976.
- [23] P. Saha and N.Zuber. An analytic study of the thermally induced two-phase flow instabilities including the effect of thermal non-equilibrium. *Int. J. Heat Mass Transfer*, 21:415–426, 1978.
- [24] J. Thome. Engineer Data Book III, chapter 13. Wolverine Tube Inc, 2006.
- [25] G. Yadigaroglu and A. Bergles. Fundamental and higher mode density-wave oscillations in two-phase flows. *Journal of heat transfer, Trans. ASME*, 94:189–195, 1972.